The effect of dipolar interactions on the thermal relaxation of magnetoferritin

2007 J. Phys.: Condens. Matter 19 456204

(http://iopscience.iop.org/0953-8984/19/45/456204)

IOP PUBLISHING JOURNAL OF PHYSICS: CONDENSED MATTER

J. Phys.: Condens. Matter **19** (2007) 456204 (6pp) doi:10.1088/0953-8984/19/45/456204

The effect of dipolar interactions on the thermal relaxation of magnetoferritin

P Southern, A P Robinson, O I Kasyutich, B Warne, A Bewick and W Schwarzacher

H H Wills Physics Laboratory, Tyndall Avenue, Bristol BS8 1TL, UK

Received 19 July 2007, in final form 6 September 2007
Published 11 October 2007
Online at stacks.iop.org/JPhysCM/19/456204

Abstract

Magnetoferritin nanoparticles consist of ferrimagnetic magnetite–maghemite surrounded by a protein shell. Thermal relaxation data for both agglomerated and well-separated magnetoferritin show clear $T\ln(t/\tau_0)$ scaling, thereby permitting a direct evaluation of the influence of magnetostatic interactions on the effective energy barrier distribution for magnetic reversal. For agglomerated magnetoferritin, the effect of the interactions is to broaden the distribution and shift its peak to lower energies, in contrast to the peak in the zero-field-cooled susceptibility, which moves to higher energies. Our result is in good agreement with earlier theoretical predictions (Iglesias and Labarta 2004 *Phys. Rev.* B **70** 144401).

Arrays of single-domain magnetic nanoparticles are important in a wide range of applications, including magnetic recording media, ferrofluids and palaeomagnetism, the study of changes in the Earth's magnetic field during geological time. Their magnetic behaviour is well understood at temperatures much greater than the blocking temperature, when magnetic relaxation is fast on the timescale of the experiment, and the nanoparticles exhibit superparamagnetic behaviour [1]. At lower temperatures, however, interactions between the particles become important and can have a significant influence on their dynamics. For example, ageing and critical slowing down have been reported for concentrated, strongly interacting systems, suggesting complex, spin-glass-like dynamics [2–4]. This complexity is a consequence of the long range of dipolar magnetostatic interactions, coupled with randomness in the position and orientation of the particles.

Most recent studies have focused on the dynamics of disordered nanoparticle arrays in zero or small applied fields [5–7]. There has been much less work on studying relaxation after the moments have been aligned by a high magnetic field. Such studies are of especial interest, however, as they not only probe the system far from any equilibrium state, but also provide a direct measure of the effective energy barrier distribution for magnetic reversal [8, 9].

0953-8984/07/456204+06$30.00

One obvious experiment is to study how varying the nanoparticle concentration to change the strength of dipolar interactions affects this effective energy barrier distribution. Surprisingly, early attempts to do just this failed to find a clear link between the energy barrier distribution and the particle concentration, leading to claims that saturation remanence measurements are inherently insensitive to these interactions [10, 11]. Other experiments found some evidence that dipolar interactions increased the effective barrier height [12], but later simulations disagreed, predicting that the interactions would shift the barrier distribution to lower energies [13]. In this paper we present unambiguous evidence that dipolar interactions do, after all, lead to significant changes in the energy barrier distribution for magnetic relaxation from saturation, and also that these changes are in good qualitative agreement with simulations [13]. We compare results from thermal relaxation experiments, where the sample is initially saturated, with zero-field-cooled susceptibility data, where the sample is initially demagnetized.

The system used for this investigation was a frozen aqueous solution of magnetoferritin particles [14]. Ferritin is an iron-storage protein which forms a hollow shell ∼2 nm thick and ∼8 nm in internal diameter enclosing a hydrated Fe(III) oxide core. Magnetoferritin is prepared by replacing the natural ferrihydrite core, which is antiferromagnetic, with a core of magnetite–maghemite (Fe_3O_4-γ-Fe_2O_3), which is ferrimagnetic [15]. It is a nearly ideal model system for studying magnetostatic interactions because the 2 nm thick protein shell prevents contact between the magnetic cores of adjacent nanoparticles, and its internal diameter places an upper limit on their size. We used reductive dissolution and dialysis to remove the ferrihydrite core from native horse spleen ferritin, resulting in empty protein shells (apoferritin), and synthesized magnetite–maghemite nanocrystals within the apoferritin following established procedures [16]. A high gradient magnetic separator was used to remove ferritin molecules where the filling with ferrimagnetic material was incomplete. Centrifugation was used to remove any ferritin clusters. It is very important to remove such clusters—the apparent lack of sensitivity to particle concentration found in some earlier saturation remanence experiments has been attributed to residual agglomeration in the ferrofluid used [17].

We studied two types of sample: as-prepared solution with a concentration of 0.4 g l^{-1} in which the magnetoferritin was well dispersed, and the same solution after the addition of $MgCl_2$ and acetone to cause aggregation. In the dispersed sample, the calculated mean interparticle separation was 130 nm, while in the aggregated sample, the ferritin molecules were in contact. For transmission electron microscopy (TEM) analysis, a small amount of solution from each sample was allowed to dry upon a carbon-coated TEM grid before applying a uranyl acetate stain to image the protein shell. Figure 1(a) suggests that the magnetoferritin in the as-prepared solution is evenly distributed. The stained protein shell (which appears bright) is intact and the electron-dense core (which appears dark) has mean diameter 7.9 nm and standard deviation 0.7 nm. The aggregated sample shown in figure 1(b) contains large areas of agglomerated particles and again the protein shell surrounding the core is visible suggesting that there was no damage to shell and core structure during aggregation.

The influence of the magnetic interactions is clearly seen in susceptibility measurements. Figure 2 presents field-cooled (FC) and zero-field-cooled (ZFC) data for well-dispersed and aggregated samples. The FC data are recorded as the sample is cooled in an applied field $H = 100$ Oe, while the ZFC data are recorded in the same applied field, as the temperature is raised at 2 K min^{-1}, after initially cooling the sample from above the blocking temperature in zero applied field. All magnetic studies were carried out using a commercial SQUID magnetometer (Quantum Design MPMS-5). Note that the peak in the ZFC susceptibility, which is proportional to the mean blocking temperature [10], increases significantly due to interactions from $T_B = 22 \pm 1$ K for well-dispersed magnetoferritin to $T_B = 28 \pm 2$ K for the aggregated sample. A similar increase has been seen in numerous other interacting systems [10, 18].

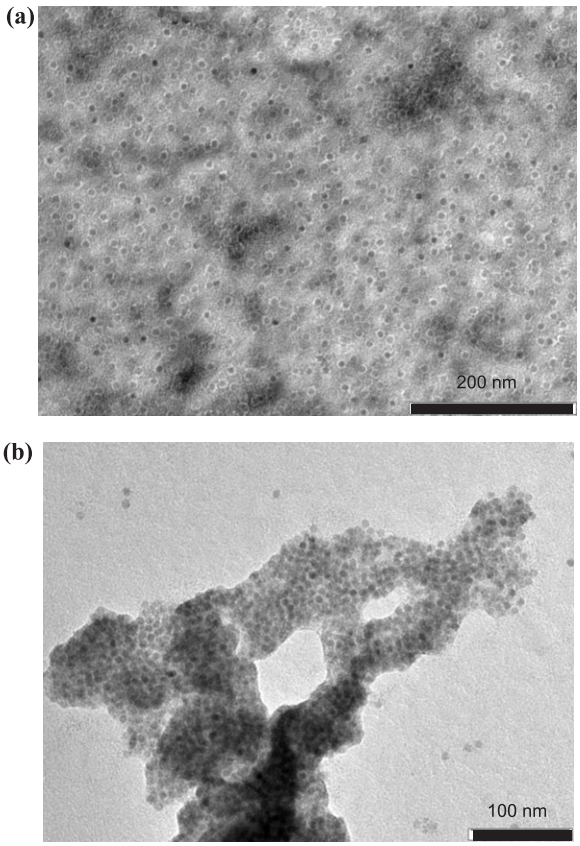

Figure 1. Transmission electron microscope (TEM) image of (a) well-dispersed and (b) aggregated magnetoferritin.

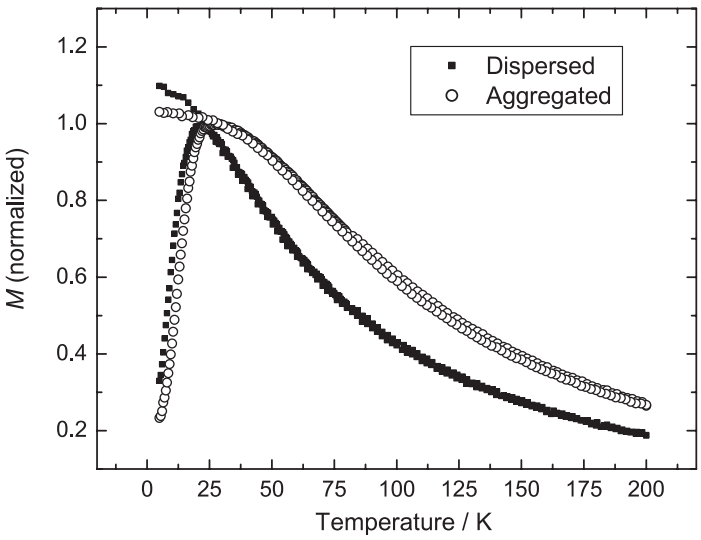

Figure 2. Field-cooled and zero-field-cooled magnetic susceptibility measured at $H = 100$ Oe for well-dispersed and aggregated magnetoferritin.

In order to study the influence of the increased interactions on relaxation following magnetic alignment, we applied a field of 5 T to samples of well-dispersed and aggregated magnetoferritin, and measured the magnetic moment M as a function of time t after

removing the field and quenching the superconducting magnet to eliminate the residual field. Measurements were made at temperatures T ranging from 2 to 28 K. Hysteresis loops showed that in all cases 5 T was sufficient to saturate the sample.

Starting with the Néel expression for the relaxation time of a single particle, $\tau(E) = \tau_0 \, \mathrm{e}^{E/k_\mathrm{B}T}$ where $1/\tau_0$ is the attempt frequency and E the energy barrier to magnetic reversal, it is easy to show that M for a system of non-interacting particles is given by

$$M = M_0 \int_0^\infty \mathrm{e}^{-t/\tau(E)} f(E) \, \mathrm{d}E, \tag{1}$$

where $f(E)\,\mathrm{d}E$ is the fraction of the moment with energy barrier between E and $E + \mathrm{d}E$. M_0 is the total moment immediately after the moment of each nanoparticle has relaxed from being parallel to the applied field to being parallel to its easy axis, and for a random distribution of easy axis directions is equal to $M_\mathrm{S}/2$, where M_S is the saturation moment. The function $\mathrm{e}^{-t/\tau(E)}$, which appears in equation (1), varies abruptly from 0 to 1 as E increases, and may be approximated as a step function with the step at $E_\mathrm{C} = k_\mathrm{B}T \ln(t/\tau_0)$, providing that the width of the energy distribution $f(E)$ is large compared to $k_\mathrm{B}T$ [19]. Equation (1) may therefore be written as

$$M = M_0 \int_{E_\mathrm{C}}^\infty f(E) \, \mathrm{d}E. \tag{2}$$

E_C is the critical value of the energy barrier for temperature T and time t, such that particles with higher barrier are blocked and particles with lower barrier are completely unblocked and do not contribute to M. Hence if M/M_0 is plotted as a function of $T \ln(t/\tau_0)$, all the data will lie on a single master curve and minus the derivative of this curve with respect to $T \ln(t/\tau_0)$ will equal $k_\mathrm{B} f(E)$ for the non-interacting system [19]. For an interacting system that exhibits $T \ln(t/\tau_0)$ scaling, $\mathrm{d}(M/M_0)/\mathrm{d}(T \ln(t/\tau_0))$ gives the effective energy barrier distribution probed while the system relaxes. Although the effective energy barrier distribution is different from the actual energy barrier distribution at any point during relaxation, simulations show that it is approximately equal to the cumulative distribution of actual energy barriers jumped by particles when they first relax [13].

Figure 3 shows that to a good approximation both the aggregated and the well-dispersed magnetoferritin obey $T \ln(t/\tau_0)$ scaling: when plotted as a function of $T \ln(t/\tau_0)$, where $\tau_0 = 10^{-9}$ s, the M/M_S data for each sample lie on a single curve. Our value of τ_0 agrees with the value for magnetoferritin obtained previously by combining Mössbauer spectroscopy with DC susceptibility measurements [20]. The scaling allows us to extract the effective energy barrier distributions by taking the derivative of the master curves in figure 3. Figure 4 shows the energy barrier distributions calculated in this manner. In each case the distribution has a single peak, in contrast to earlier studies of native ferritin where the energy barrier distribution consisted of a log-normal and an exponentially decaying component, thought to be associated with multiple interacting entities within each ferritin particle [8]. Demonstrating the self-consistency of our measurements, the area under the energy barrier distribution curve is the same in the presence and absence of interactions[1].

Aggregating the magnetoferritin clearly leads to significant changes. In particular, the increase in the strength of the magnetostatic interactions makes the peak in the energy barrier distribution move to a lower energy and become broader. The greater weight of lower energy barriers indicates that the overall effect of interactions on relaxation from saturation is demagnetizing. The demagnetizing effect of the interactions also explains the negative deviations from the Wohlfarth relationship found for this and similar systems when comparing

[1] The area is approximately equal to 0.5 rather than 1.0 because the data is normalized to the saturation moment at 5 K, rather than to M_0.

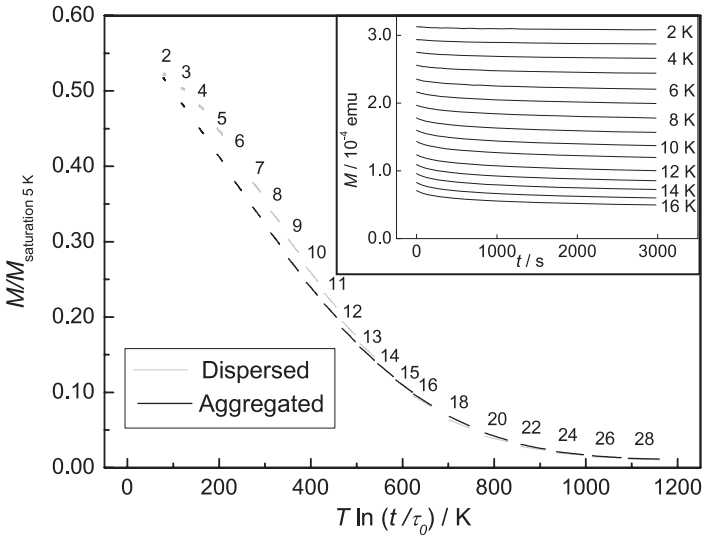

Figure 3. Thermal relaxation of the magnetic moment M for well-dispersed and aggregated magnetoferritin following saturation in an applied field of 5 T, normalized to M_S, the saturation moment measured at $T = 5$ K. The figure next to each data segment indicates the temperature in kelvins at which that data was recorded. Data plotted as a function of $T \ln(t/\tau_0)$ where $\tau_0 = 10^{-9}$ s. Inset: a selection of this data (for aggregated magnetoferritin and temperatures between 2 and 16 K) plotted as a function of t (s).

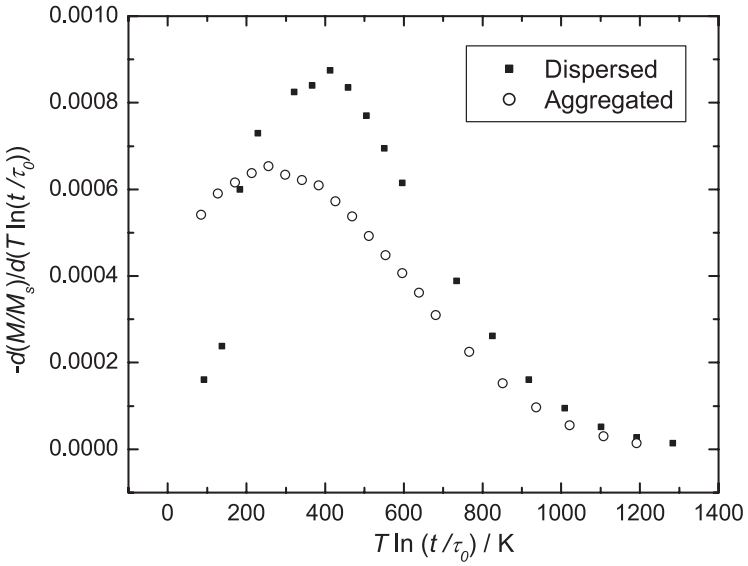

Figure 4. The data of figure 3 differentiated with respect to $T \ln(t/\tau_0)$. This curve gives the effective energy barrier distribution $f(E)$, where $f(E)\,\mathrm{d}E$ is the fraction of the moment with effective energy barrier between E and $E + \mathrm{d}E$.

the magnetizing and demagnetizing remanence [21–23]. Our result is in excellent qualitative agreement with simulations (compare figure 4 with figure 8 of [13]), even though the latter modelled a one-dimensional chain of particles rather than a three-dimensional distribution as studied here.

Given that the changes in the effective energy barrier distribution between the well-dispersed and aggregated samples suggest that interactions facilitate magnetic reversal, it might appear surprising that the peak blocking temperature T_B increases for the aggregated sample (figure 2), because an increase in T_B suggests that interactions hinder thermally activated reversal. However, there is a crucial difference between the ZFC and the time-dependent M measurements, which is that the former start from a demagnetized state, while the latter start with the sample magnetically saturated. There is no contradiction between the energy barriers jumped during relaxation from the saturated state being lower for an interacting system and the energy barriers blocking magnetic reversal once in the demagnetized state being higher. Indeed, the blocking effect of interactions is consistent with the spin-glass-like dynamics observed in previous experiments [2–4] on demagnetized, strongly interacting systems[2].

To summarize, we have used well-dispersed and aggregated samples of the modified iron-storage protein magnetoferritin as a model system for studying the effects of magnetostatic interactions on magnetic thermal relaxation from saturation. Clear $T\ln(t/\tau_0)$ scaling enabled us to calculate the (effective) energy barrier distribution in each case. In contrast to earlier measurements [10–12], we found that interactions lead to both a decrease in the peak energy and to a broadening of the distribution. This result strongly supports the applicability of relatively simple simulations [13].

Acknowledgment

This work was supported by the UK Engineering and Physical Sciences Research Council.

References

[1] Néel L 1949 *Ann. Geophys.* **5** 99
[2] Jonsson T, Mattsson J, Djurberg C, Khan F A, Nordblad P and Svedlindh P 1995 *Phys. Rev. Lett.* **75** 4138
[3] Djurberg C, Svedlindh P, Nordblad P, Hansen M F, Bødker F and Mørup S 1997 *Phys. Rev. Lett.* **79** 5154
[4] Mamiya H, Nakatani I and Furubayashi T 1999 *Phys. Rev. Lett.* **82** 4332
[5] Woods S I, Kirtley J R, Sun S and Koch R H 2001 *Phys. Rev. Lett.* **87** 137205
[6] Poddar P, Telem-Shafir T, Fried T and Markovich G 2002 *Phys. Rev.* B **66** 060403(R)
[7] Luis F, Petroff F, Torres J M, García L M, Bartolomé J, Carrey J and Vaurès A 2002 *Phys. Rev. Lett.* **88** 217205
[8] St Pierre T G, Gorham N T, Allen P D, Costa-Krämer J L and Rao K V 2001 *Phys. Rev.* B **65** 024436
[9] Gorham N T, Woodward R C, St Pierre T G, Terris B D and Sun S 2005 *J. Magn. Magn. Mater.* **295** 174
[10] O'Grady K, El-Hilo M and Chantrell R W 1993 *IEEE Trans. Magn.* **29** 2608
[11] Hayashi M, Susa M and Nagata K 1997 *J. Magn. Magn. Mater.* **171** 170
[12] Mørup S, Bødker F, Hendriksen P V and Linderoth S 1995 *Phys. Rev.* B **52** 287
[13] Iglesias Ó and Labarta A 2004 *Phys. Rev.* B **70** 144401
[14] Meldrum F C, Heywood B R and Mann S 1992 *Science* **257** 522
[15] Gider S, Awschalom D D, Douglas T, Mann S and Chaparala M 1995 *Science* **268** 77
[16] Wong K K W, Douglas T, Gider S, Awschalom D D and Mann S 1998 *Chem. Mater.* **10** 279
[17] Pike C R, Roberts A P and Verosub K L 2000 *J. Appl. Phys.* **88** 967
[18] Luo W, Nagel S R, Rosenbaum T F and Rosensweig R E 1991 *Phys. Rev. Lett.* **67** 2721
[19] Labarta A, Iglesias Ó, Balcells Ll and Badia F 1993 *Phys. Rev.* B **48** 10240
[20] Moskowitz B M, Frankel R B, Walton S A, Dickson D P E, Wong K, Douglas T and Mann S 1997 *J. Geophys. Res.* **102** 22671
[21] Wohlfarth E P 1958 *J. Appl. Phys.* **29** 595
[22] Henkel O 1964 *Phys. Status Solidi* **7** 919
[23] Mitchler P D, Roshko R M, Dahlberg E D and Moskowitz B M 1999 *IEEE Trans. Magn.* **35** 2029
[24] Mathieu R, Jönsson P, Nam D N H and Nordblad P 2001 *Phys. Rev.* B **63** 092401

[2] Our system was not sufficiently strongly interacting to exhibit a detectable memory effect for a ZFC process with a stop during cooling under zero field, for example, see [24].